A R C H I V E S O F M E T A L L U R G Y A N D M A T E R I A L S
Volume 58 2013 Issue 1
DOI: 10.2478/v10172-012-0146-9

M. GWOŹDZIK*, Z. NITKIEWICZ*

ANALYSIS OF CRYSTALLITE SIZE AND LATTICE DEFORMATIONS CHANGES IN AN OXIDE LAYER ON P91 STEEL

ANALIZA ZMIAN WIELKOŚCI KRYSTALITÓW I ODKSZTAŁCEŃ SIECIOWYCH W WARSTWIE TLENKÓW NA STALI P91

The paper contains results of studies on X-ray diffraction analysis XRD (studying the phase composition, crystallite sizes and lattice deformations) of oxide layers on P91 steel, operated for a long time at an elevated temperature (T = 535°C, t = 70,000 h). X-ray studies were carried out on the inner surface of a tube, and then the layer surface was polished down to 3.5 μm and the diffraction measurements were performed again to determine individual oxide layers.

It has been found that a three-zone oxide layer is formed as a result of long-term operation of P91 steel at the temperature of 535°C. Hematite occurs on the inner surface of the tube. Then magnetite appears below hematite. Going deeper into the layer there is a spinel, i.e. a mixture of magnetite and chromite.

A visible decay of total intensity for Fe_2O_3 is observed already at the polishing depth of 3.5 μm. In the case of Fe_3O_4 and $FeCr_2O_4$ an increase in total intensity is observed already from 7 μm, what manifests in narrowing the diffraction line and hence in increasing the crystallites size and in the relaxation of stresses in this oxide layer.

The broadening of a diffraction line caused by a small size of crystallites is expressed by the Scherrer relationship. Instead, the β_z broadening resulting from lattice distortions (relaxation of stresses) was determined from the Taylor relationship.

Keywords: crystallite sizes, P91 steel, oxide layers

Praca zawiera wyniki badań dotyczących rentgenowskiej analizy dyfrakcyjnej XRD (badanie składu fazowego, wielkości krystalitów i odkształceń sieciowych) warstw tlenkowych na stali P91 długotrwale eksploatowanej w podwyższonej temperaturze (T=535°C, t=70000h). Badania rentgenograficzne przeprowadzono na powierzchni wewnętrznej rury, następnie powierzchnię warstwy spolerowywano na głębokość 3,5 μm i ponownie wykonywano pomiary dyfrakcyjne w celu określenia poszczególnych warstw tlenkowych.

Stwierdzono, że w wyniku długotrwałej eksploatacji stali P91 w temperaturze 535°C powstaje trójstrefowa warstwa tlenków. Na powierzchni wewnętrznej rury występuje hematyt. Następnie poniżej hematytu pojawia się magnetyt. Idąc dalej w głąb warstwy występuje spinel, tj. mieszanina magnetytu i chromitu.

Widoczny zanik intensywności całkowitej dla Fe_2O_3 obserwuje się już na głębokości polerowania 3,5 μm. W przypadku Fe_3O_4 i $FeCr_2O_4$ od 7 μm obserwuje się już wzrost intensywności całkowitej, co przejawia się zwężeniem linii dyfrakcyjnej, a tym samym zwiększeniem wielkości krystalitów i relaksacją naprężeń w tej warstwie tlenków.

Poszerzenie linii dyfrakcyjnej spowodowane małą wielkością krystalitów wyraża się zależnością Scherrera. Natomiast zwężenie wynikające ze zniekształceń sieciowych (relaksacji naprężeń) wyznaczono z zależności Taylora.

1. Introduction

X-ray methods are widely used to study the texture, residual stress and crystallite size determination [1-7].

The size of polycrystalline body crystallites, determined by means of X-ray methods, is a statistical quantity. The influence of crystallite size on the diffraction reflections nature and intensity is the physical basis of those methods.

Methods based on the analysis of diffraction line profile are used to determine the size of crystallites smaller than 100 nm and of lattice distortions. The methods in which the line width is used for measurements are the approximation methods and the methods using full information on the reflection profile are methods of harmonic analysis and analysis of variance. Methods based on the diffraction reflection width are frequently used due to the speed of results obtaining [8].

The broadening of a diffraction line caused by a small size of crystallites is expressed by the Scherrer relationship [5-7]:

$$\beta_k = K\lambda/D_{hkl}cos\theta \tag{1}$$

where:

β_k – reflection width depending on the crystallite size, rad

K – constant (~1),

λ – radiation wavelength, nm

D_{hkl} – crystallite size in the direction normal to (hkl), nm

θ – Bragg angle, rad

* CZĘSTOCHOWA UNIVERSITY OF TECHNOLOGY, INSTITUTE OF MATERIALS ENGINEERING, 42-201 CZĘSTOCHOWA, 19 ARMII KRAJOWEJ AV., POLAND

TABLE 1

Chemical composition of examined steel, wt %

acc. to	Chemical composition, %											
	C	Si	Mn	P	S	Cr	Mo	Ni	V	Al	Nb	N
analysis	0.10	0.29	0.49	0.012	0.002	8.66	0.97	0.29	0.19	0.005	0.07	0.52
PN-EN 10028-2:2010 [9]	0.08-0.12	max. 0.50	0.30-0.60	max. 0.020	max. 0.005	8.00-9.50	0.85-1.05	max. 0.30	0.18-0.25	max. 0.04	0.06-0.1	0.03-0.07

Instead, the β_z broadening resulting from lattice distortions (originating from type II stresses) may be determined from the Taylor relationship [5]:

$$\beta_z = 4\varepsilon \cdot tg\theta \tag{2}$$

where:

ε – lattice deformations,

θ – Bragg angle, rad

The total broadening of a diffraction line is a sum of β_k and β_z broadenings, then the equation described by a Cauchy type function has the form:

$$\beta \cdot cos\theta = \lambda/D + 4\varepsilon \cdot sin\theta \tag{3}$$

β is determined from relationship:

$$\beta = B - b \tag{4}$$

where:

B – {hkl}reflection width of the specimen studied,

b – standard's reflection width (powders of studied oxides were used as the standard).

The crystallite size and the value of lattice distortions was determined through the determination of $\beta \cdot \cos\theta$ versus $\sin\theta$ relationship for the three main reflection of oxides studied and plotting a straight line using a linear regression method.

2. Material and experimental methods

The material studied comprised specimens of X10CrMoVNb9-1 (P91) steel taken from a fresh steam pipeline operated at the temperature of 535°C during 70,000 hours. The analysis of steel chemical composition was carried out using spark emission spectroscopy on a Spectro spectrometer (Table 1).

The oxide layer was studied on a cross-section at the inner surface of the tube wall (Fig. 1).

Microscopic examinations of the oxide layer were performed using an Olympus GX41 optical microscope.

X-ray (XRD) measurements were performed on a Seiffert 3003T/T X-ray spectrometer with a cobalt target tube (λ_{Co} =0.17902nm).

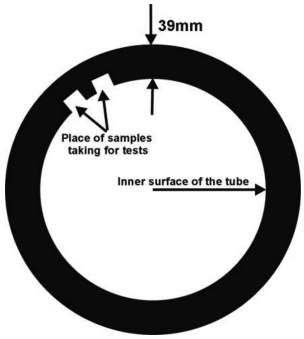

Fig. 1. Place of samples taking for tests

3. Results

X-ray studied were carried out on the inner surface of the tube and after polishing the layer down to around 3.5 μm. X-ray measurements revealed differences in the phase composition of oxide layers. X-ray diffraction patterns, starting from the oxide layer towards the native material, are specified in Fig. 2a.

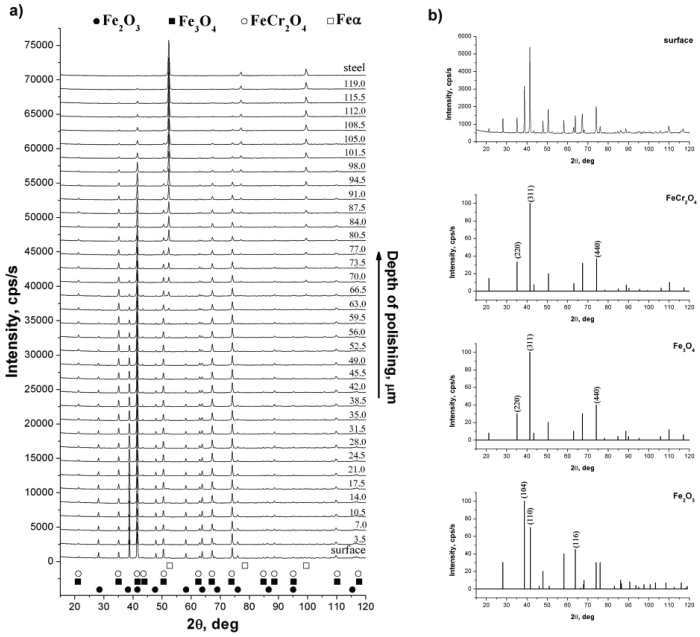

Fig. 2. X-ray diffraction patterns from the oxides layer obtained by means of XRD technique (a) [10], standards corresponding to individual oxides, in which the main reflections originating from three planes are marked (b)

Three zones have been distinguished in the oxides layer formed, which was presented in paper [10]. Hematite

(Fe_2O_3) occurs at the surface, then magnetite (Fe_3O_4), under which a spinel, i.e. a mixture of magnetite and chromite (Fe_3O_4+$FeCr_2O_4$) exists (Fig. 3).

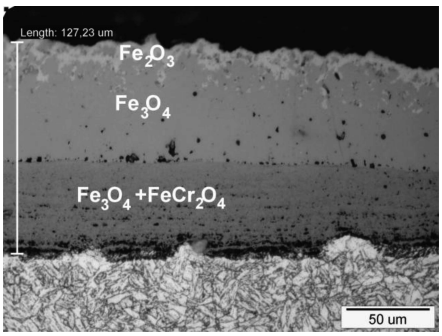

Fig. 3. Cross-section of the oxides layer formed on the steel examined

Diffraction patterns from oxide layers obtained via XRD measurements represent reflections originating from three oxides, Fe_2O_3, Fe_3O_4, and $FeCr_2O_4$. The main reflections originating from three planes (104), (110), (116) for Fe_2O_3 and (311), (440), (220) common for Fe_3O_4 and $FeCr_2O_4$ have been carefully analysed because of close values of interplanar spacings (Fig. 2b).

To separate the overlapping peaks originating from Fe_2O_3, Fe_3O_4 and $FeCr_2O_4$ the diffraction patterns were subject to numerical processing, enabling those peaks separation using the Gauss method. An example of X-ray diffraction pattern with separated peaks originating from (311) plane of Fe_3O_4 and $FeCr_2O_4$ and (110) of Fe_2O_3 is presented in Fig. 4.

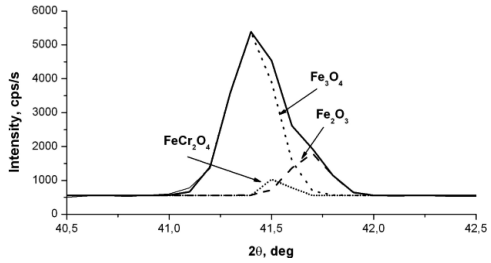

Fig. 4. X-ray diffraction pattern with separated peaks originating from Fe_2O_3, Fe_3O_4 and $FeCr_2O_4$

The total intensity of reflections originating from planes (104), (110), (116) for Fe_2O_3 suddenly decreases already after polishing down to the depth of 3.5 μm (Fig. 5a). Then there is a gradual decline of total intensity originating from only two planes, (104) and (116). The total intensity for those plane decays entirely at the polishing depth of 80 μm. Such a large thickness of Fe_2O_3 layer may result from a different thickness of oxide layers, presented in paper [10], where the oxide layer thickness was determined in the narrowest place as 40.64 μm and in the widest as 122.24 μm. The existence of Fe_2O_3 to a depth of around 80 μm may be explained by the fact, that where the Fe_2O_3 layers have already been polished in the largest range, in the narrowest Fe_2O_3 range they only started to occur. Hansson et al in paper [11] identified Fe_2O_3 to the depth of 3.0 μm from the surface. They carried out the oxidation at the temperature of 600°C in Ar-46% +H_2O during 336 hours on TP 347H FG steel.

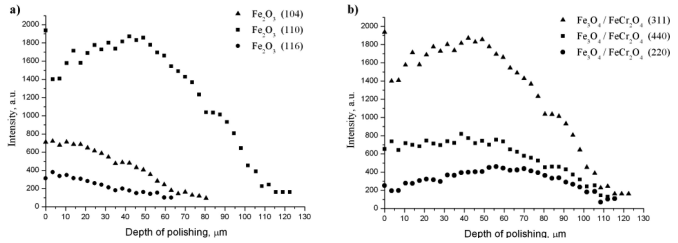

Fig. 5. Total intensity of three main reflections versus the depth of polishing: a) Fe_2O_3, b) Fe_3O_4 / $FeCr_2O_4$

In the case of (110) plane for Fe_2O_3 the total intensity increases from 7.0 μm, resulting from the overlapping of reflections originating from this plane with the reflection originating from (311) plane for Fe_3O_4 and $FeCr_2O_4$, which starts occurring at this depth of polishing. The total intensity for reflections originating from planes (311), (440), (220) increases gradually to 55 μm. Then the reflections originating from those planes versus the depth of polishing gradually decay and at a depth of around 122 μm those reflections decay entirely.

For Fe_2O_3 the total intensity of diffraction peaks originating from planes (104) and (116) declines (Fig. 5a) and at the same time the diffraction line is broadened (Fig. 6a), which is caused by decreasing crystallite sizes (Fig. 7). Instead, an inverse relationship has been observed for Fe_3O_4 and $FeCr_2O_4$. In this case the total intensity of reflections originating from planes (311), (440) and (220) increases (Fig. 5b) and at the same time the diffraction line is narrowed (Fig. 6b), which is caused by increasing crystallite sizes and relaxation of stresses in this oxide layer (Fig. 8, 9).

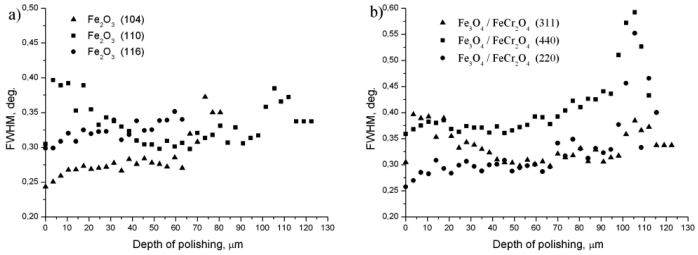

Fig. 6. Half-intensity width of three main reflections versus the depth of polishing: a) Fe_2O_3, b) Fe_3O_4 / $FeCr_2O_4$

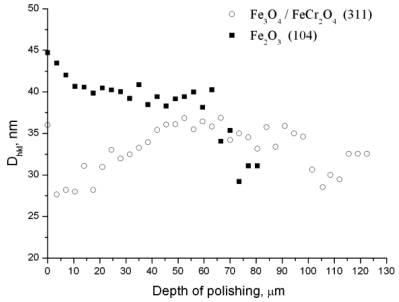

Fig. 7. Determination of crystallite size D_{hkl} for main peaks Fe_3O_4 / $FeCr_2O_4$ and Fe_2O_3

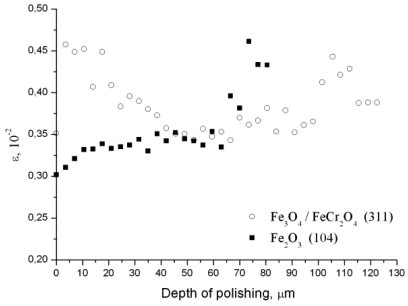

Fig. 8. Determination of lattice deformations ε based on the position and half-intensity width for main Fe_3O_4 / $FeCr_2O_4$ and Fe_2O_3 peaks

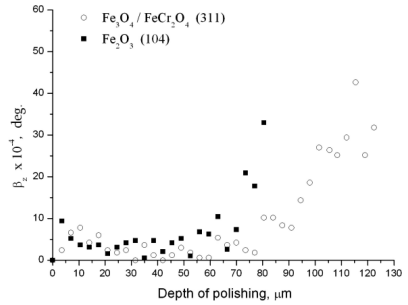

Fig. 9. Narrowing resulting from the relaxation of stresses determined for main Fe_3O_4 / $FeCr_2O_4$ and Fe_2O_3 peaks

4. Summary of results

The layer of oxides formed on P91 high-chromium steel operated at the temperature of 535°C during 70,000 hours consists of three different layers. Hematite (Fe_2O_3), originating on the oxide – flowing medium interface, exists in this layer. Magnetite (Fe_3O_4) exists under this layer and then there is a spinel below, i.e. a mixture of magnetite and chromite (Fe_3O_4+$FeCr_2O_4$).

A visible decay of total intensity for Fe_2O_3 is observed already after polishing down to around 3.5 μm from the surface. In the case of Fe_3O_4 and $FeCr_2O_4$ an increase in total intensity is observed already from 7 μm as well as a narrowing of the diffraction line and hence an increase in crystallites size and the relaxation of stresses in this oxide layer.

Crystallites originating from Fe_2O_3 are larger than Fe_3O_4 / $FeCr_2O_4$ (Fig. 7), which can substantially affect the structure and mechanical properties of the layer studied. Papers [12, 13] have shown that the outer layer of oxides is more brittle and susceptible to cracking than the Fe_3O_4+$FeCr_2O_4$ layer. An excessive chipping and spalling of the oxide layer is unfavourable, because it can cause erosion within the turbine. The chipping oxides can also plug the bore of superheater and other steam pipes, causing a local overheating, which frequently results in their bursting.

REFERENCES

[1] A. Borbely, J.H. Driver, Archives of Metallurgy and Materials **50**, 1, 65-76 (2005).
[2] J. Mizera, Z. Pakieła, K.J. Kurzydłowski, Archives of Metallurgy and Materials **50**, 2, 395-402 (2005).
[3] M. Gwoździk, Z. Nitkiewicz, Inżynieria Materiałowa, 6, 1009-1012 (2008).
[4] Z. Nitkiewicz, M. Gwoździk, Inżynieria Materiałowa, 3, 229-232 (2006).
[5] D. Oleszak, A. Olszyna, Kompozyty **4**, 284-288 (2004).
[6] A. Malek, B. Projjal, Journal of Alloys and Compounds **491**, 581-583 (2010)
[7] R. Tahmasebi, M. Shamanian, M.H. Abbasi, M. Panjepour, Journal of Alloys and Compounds **472**, 334-342 (2009).
[8] Z. Bojarski, E. Łągiewka, Rentgenowska analiza strukturalna. Wydawnictwo Uniwersytetu Śląskiego, 324-332 (1995).
[9] PN-EN 10028-2:2010, Polish Standard (Flat products made of steels for pressure purposes – Part 2: Non-alloy and alloy steels with specified elevated temperature properties).
[10] M. Gwoździk, Inżynieria Materiałowa **2** (180), 128-131 (2011).
[11] A.N. Hansson, K. Pantleon, F.B. Grumsen, M.A.J. Somers, Oxid Met **73**, 289-309 (2010).
[12] M. Gwoździk, Inżynieria Materiałowa **4** (182), 432-434 (2011).
[13] M. Gwoździk, Z. Nitkiewicz, Inżynieria Materiałowa **4** (182), 435-438 (2011).

Received: 10 December 2011.